

# Self-Assembled Monolayer of Carboxyl-Terminated Poly(amido amine) Dendrimer

Masahiro Ito<sup>1</sup> and Toyoko Imae<sup>1,2,\*</sup>

<sup>1</sup>Graduate School of Science and <sup>2</sup>Research Center for Materials Science, Nagoya University, Chikusa, Nagoya 464-8602, Japan

Adlayer formation and adsorption structure of 2.5th-generation poly(amido amine) dendrimer with carboxyl-terminated groups on solid substrates were investigated by atomic force microscopy, surface plasmon resonance spectroscopy, and surface enhanced infrared absorption spectroscopy. Dendrimer molecules are not uniformly adsorbed on solid surface but form aggregates with a width of ~100 nm and a height less than 1 nm. Adsorption reaches in equilibrium at 100 ~ 1000 sec, depending on the dendrimer concentration. The adsorption-desorption process is considerably reproducible and repeatable. Although the adsorption at equilibrium increases with dendrimer concentration and reaches maximum at neutral pH, monolayer is always maintained after the desorption with solvent. This indicates the formation of self-assembled monolayer. Such monolayer is preserved even at the variation of pH. Although most carboxylates are protonated at acidic pH, small amount of carboxylate remains even at acidic pH. The adsorption structure of dendrimer was illustrated.

**Keywords:** Poly(Amido Amine) Dendrimer, Carboxyl Terminal, Self-Assembled Monolayer, Atomic Force Microscopy, Surface Plasmon Resonance Spectroscopy, Infrared Absorption Spectroscopy, Surface Enhanced Infrared Absorption Spectroscopy, Adsorption Layer. Copyright: American Scientific Publishers

## 1. INTRODUCTION

One of advantages of dendrimers is the possible utilization as building blocks in the self-assembly construction.<sup>1-3</sup> The self-assembly of dendrimers is mediated by hydrogen bond, electrostatic interaction, hydrophobic interaction, metal complexation, and so on. As a result, dendrimer aggregates in solutions, dendrimer liquid crystals, metal-dendrimers, dendrimer films, etc., can be formed. Many investigations have been reported, associating with the dendrimer-constituted films such as mono- or multiadlayers of dendrimers on solid substrates,<sup>4-7</sup> self-assembled composite multilayer films from dendrimers with different terminal groups and from dendrimer and linear polymer on solid substrates,<sup>8,9</sup> covalent and adsorbed attachment of dendrimers on self-assembled monolayer (SAM),<sup>10-12</sup> mixed monolayer of dendrimers with alkylthiols on gold,<sup>13</sup> chemisorbed adlayer of dendron thiol on gold,<sup>14,15</sup> spread films of dendrimers and dendrons at air/water interface and their transfer films on solid substrates,<sup>7,16-18</sup> ordered array of metal-initiated self-assembly from dendrimers and bridging ligands,<sup>19</sup> and patterned films of dendrimers.<sup>20</sup>

The formation of SAM depends on the combination of adsorbate and substrate. It is well known that thiol derivatives are most probable as SAM-forming molecules on gold substrate. Some investigators reported the formation and properties of dendron thiol SAM.<sup>14,15</sup> The binding of thiol on gold is strong and, therefore, thiol SAM is very stable. On the other hand, one of authors and her collaborators have found that carboxyl derivatives, tetraacidic and diacidic protoporphyrins, formed SAM on substrates, and they discussed the molecular orientation in SAM.<sup>21</sup> This suggests that carboxyl derivatives also can form stable SAM. In the present work, the adlayer formation and the adlayer-forming process of carboxyl-terminated poly(amido amine) (PAMAM) dendrimer on solid substrates were investigated using atomic force microscopy (AFM), surface plasmon resonance (SPR) spectroscopy and surface enhanced infrared absorption spectroscopy (SEIRAS). The stable SAM formation of carboxyl derivative of dendrimers is confirmed.

## 2. EXPERIMENTAL DETAILS

2.5th generation (G2.5) carboxyl-terminated PAMAM dendrimer and G4 amine-terminated PAMAM dendrimer (Chart 1) were purchased as a 10 wt% methanol solution

\*Author to whom correspondence should be addressed.

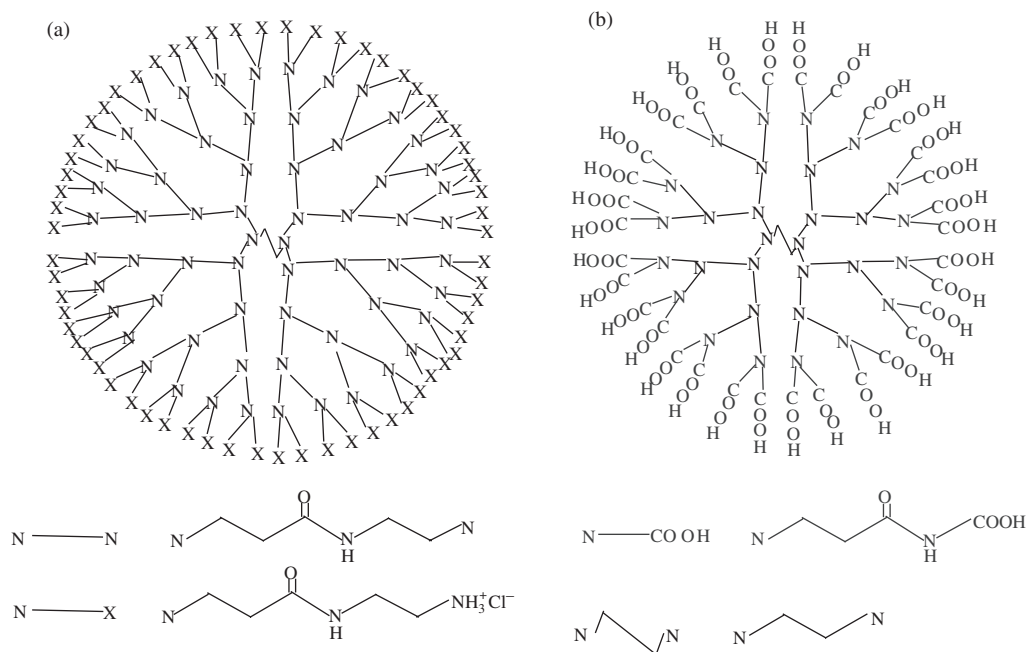


**Chart 1.** Chemical structures of dendrimers. (a) G4 amine hydrochloride-terminated poly(amido amine) dendrimer; (b) G2.5 carboxylic acid-terminated poly(amido amine) dendrimer.

from Aldrich. The solvent was removed and then the residual was dissolved in water. Other reagents were commercial grade. The pH of aqueous solutions of dendrimer was adjusted by adding an aliquot of concentrated HCl or a saturated solution of NaOH. All aqueous solutions were prepared using ultra pure water (Millipore milli-Q labo).

AFM observation was carried out on a Digital Instruments NanoScope III apparatus. Freshly-cleaved mica was used as a substrate. A Bio-Rad FTS 575C FT-IR spectrometer was used for measuring IR spectra. Transmission SEIRAS was measured on gold island-evaporated  $\text{CaF}_2$  windows. Detail of the measurements is described elsewhere.<sup>22</sup> The specimens for AFM and IR experiments were prepared by immersing the substrates into aqueous solutions of dendrimers and drying.

SPR spectroscopic measurements were performed on a Nippon Laser & Electronics biosensor analytical system. The flow cell equipped with gold substrate was used. Reflectance versus incidence angle curves were fitted using a standard Fresnel theory.<sup>23</sup> By using known complex dielectric constants  $\epsilon$  (suffix r and i: real and imaginary parts, respectively) of silicon prism ( $\epsilon_r = 2.29$ ,  $\epsilon_i = 0$ ) and aqueous medium ( $\epsilon_r = 1.77$ ,  $\epsilon_i = 0$ ), the parameters for the gold layer were evaluated from the best fit to the observed SPR spectrum from a system without an adlayer, and they were  $\epsilon_r = -13.3$ ,  $\epsilon_i = 2.30$  and thickness = 43 ~ 44 nm. Then the dielectric constant ( $\epsilon_r = 1.86$ ,  $\epsilon_i = 0$ ) and the thickness of adlayer were evaluated from the best fit to the SPR spectrum of an adlayer. Detail of the SPR measurements and analyses is described elsewhere.<sup>6b</sup>

### 3. RESULTS AND DISCUSSION

AFM image and its section analysis of carboxyl-terminated PAMAM dendrimer adsorbed on mica at 5 min immersion in a dendrimer solution (0.01 wt%) are compared to those of amine-terminated PAMAM dendrimer in Figure 1. Carboxyl-terminated dendrimer formed domains of about 1 nm height difference in maximum and about 100 nm width. This profile of adsorption surface was different from flatter but irregularly bumpy adsorption surface of amine-terminated dendrimer.

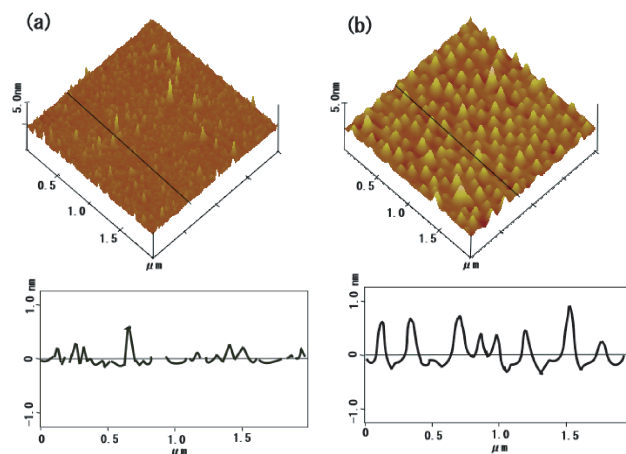


**Fig. 1.** Atomic force microscopic images of dendrimers adsorbed from aqueous solutions (0.01 wt%) for 5 min. Their section analyses are drawn in the bottom. (a) G4 amine hydrochloride-terminated poly(amido amine) dendrimer; (b) G2.5 carboxylate-terminated poly(amido amine) dendrimer.

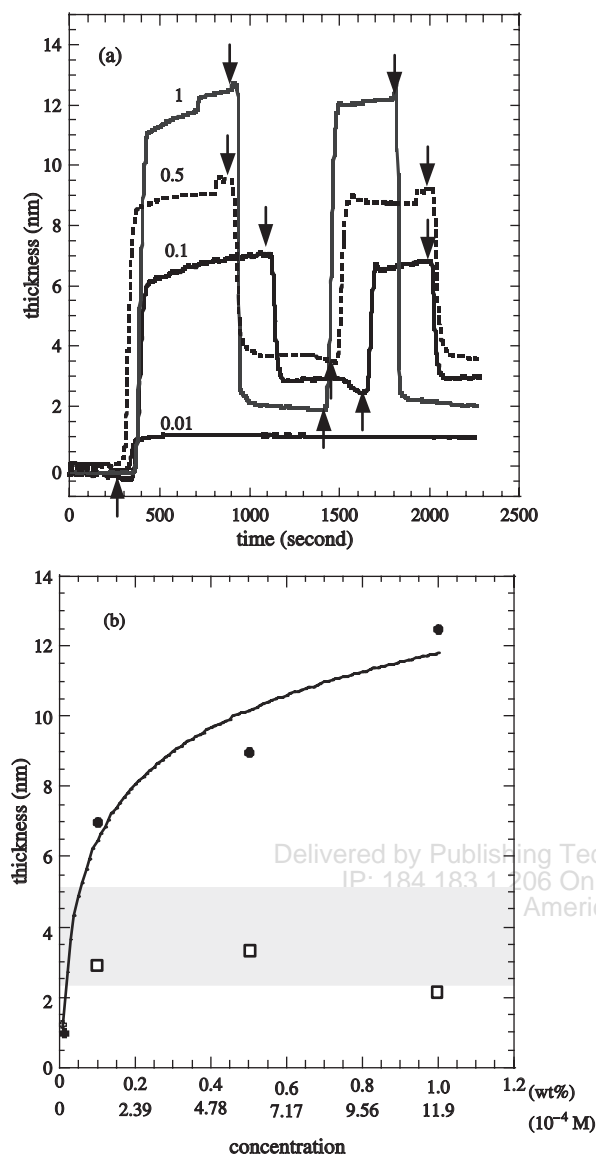


**Fig. 2.** Adsorption-desorption profile as a function of time at different dendrimer concentrations (a) and adlayer thickness at adsorption and desorption equilibrium as a function of dendrimer concentration (b) for aqueous solutions of G2.5 carboxyl-terminated poly(amido amine) dendrimer. Numbers in the top figure denote dendrimer concentrations in unit of wt%. The symbols,  $\uparrow$  and  $\downarrow$ , in the top figure denote start of adsorption and desorption, respectively. In the bottom figure, filled circle and opened square denote adlayer thickness at adsorption and desorption equilibrium, respectively. The dark tie at 2.3 ~ 5.1 nm thickness denotes the calculated dendrimer size width. A solid curve was drawn to be visual.

An adsorption-desorption profile at various concentrations of carboxyl-terminated PAMAM dendrimer was observed as a function of time by SPR. As shown in Figure 2a, the adsorption process depended on dendrimer concentration but the equilibrium reached at 100–1000 sec. While desorption in water also reached in equilibrium at similar time scale, the film thickness at desorption equilibrium was finite but not nil. The adsorption-desorption process was reproducible and repeatable. As seen in

Figure 2b, the adsorption at equilibrium on adsorption process increased with dendrimer concentration and the adsorption layer reached ~12 nm at 1 wt%. On the other hand, equilibrium film thickness on desorption process was about 3 nm, which was independent of adsorption and within the calculated dendrimer size width (see Fig. 2b). This indicates the formation of the self-assembled monolayer after desorption process. Then the adlayer thickness on adsorption process at 1 wt% is 3–4 times of a monolayer thickness. Conversely, adlayer thickness (~1.5 nm) adsorbed from a 0.01 wt% dendrimer solution was thinner than monolayer thickness. This means that the 0.01 wt% concentration is too diluted to accomplish whole monolayer and only half surface of substrate is covered by monolayer.

The increase in adlayer thickness of carboxyl-terminated PAMAM dendrimer from aqueous solution (0.01 wt%) is shown in Figure 3 as a function of adsorption time. The adsorption was rapidly attained up to 300 sec and involved slight decrease with time. The adsorption kinetics was analyzed on the basis of two adsorption models: One is simple Langmuir model and another is two-step adsorption model.<sup>24</sup> The calculated curves from both models fit well to the observed one, but the two-step model was slightly better than the Langmuir model. The excessively adsorbed molecule may desorb or the rearrangement of the adsorbed molecule may occur. Similar two-step adsorption profile was previously reported.<sup>24, 25</sup>

Figure 4a is the SPR results of time-dependent adsorption/desorption at different solution pHs. Both adsorption and desorption processes are fast as well as a case of concentration dependence. The film thickness after adsorption and desorption equilibrium is given as a function of pH in Figure 4b. The film thickness at adsorption equilibrium was maximum (more than 25 nm) at ~ pH 6. This value is

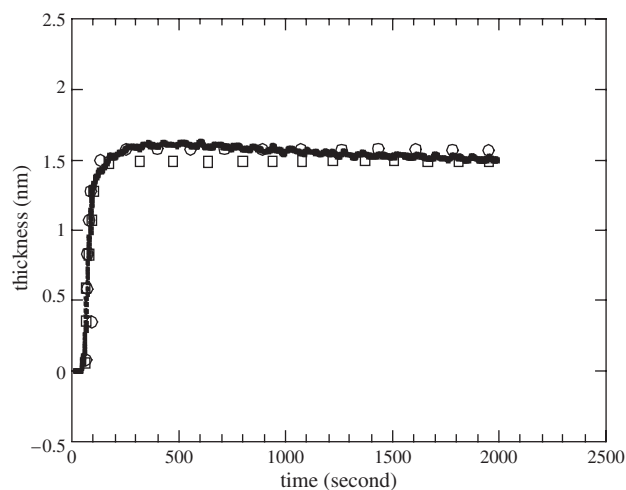


**Fig. 3.** Adlayer thickness variation as a function of adsorption time for an aqueous solution (0.01 wt%) of G2.5 carboxyl-terminated PAMAM dendrimer. Calculation:  $\square$  Langmuir adsorption kinetics;  $\circ$ , two-step adsorption kinetics.

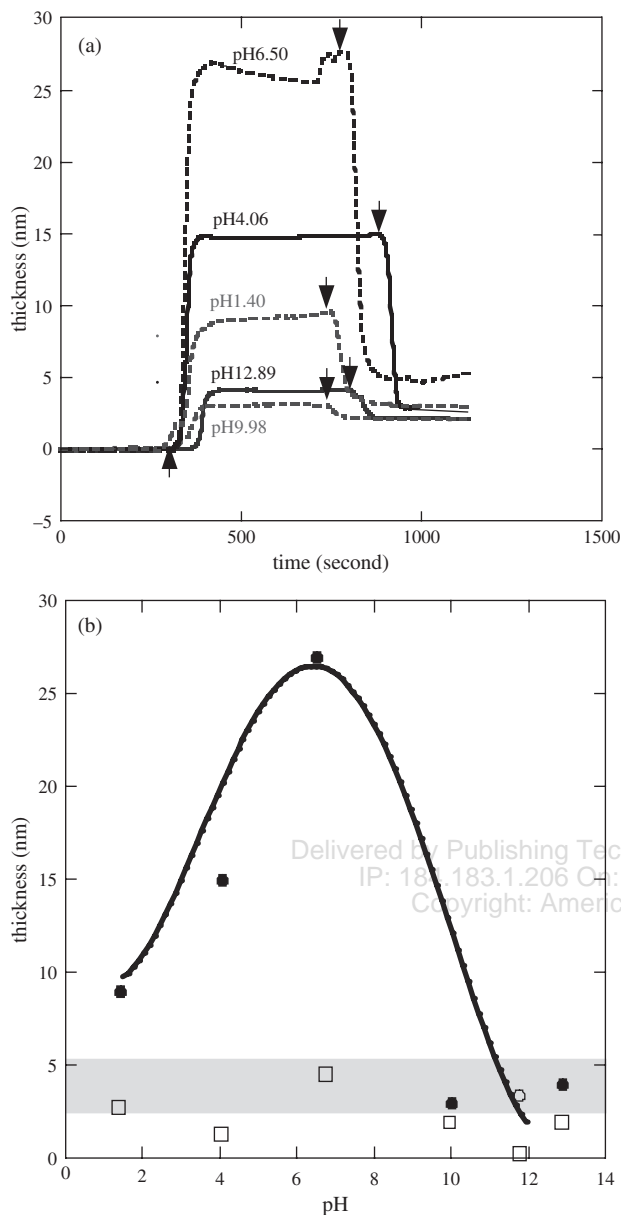


**Fig. 4.** Adsorption-desorption profile as a function of time at different pHs (a) and adlayer thickness at adsorption and desorption equilibrium as a function of pH (b) for aqueous solutions (0.1 wt%) of G2.5 carboxyl-terminated poly(amido amine) dendrimer. The symbols,  $\uparrow$  and  $\downarrow$ , in the top figure denote start of adsorption and desorption, respectively. In the bottom figure, filled circle and opened square denote adlayer thickness at adsorption and desorption equilibrium, respectively. The dark tie at 2.3 ~ 5.1 nm thickness denotes the calculated dendrimer size width. A solid curve was drawn to be visual.

larger than 7 ~ 9 times of monolayer. The adsorption maintains ~10 nm thickness at pH 2, but it is very low (~3 nm) at alkaline pH. However, the film thickness at desorption equilibrium was only monolayer level at whole pH region.

Figure 5 shows SEIRA spectra of amine- and carboxyl-terminated PAMAM dendrimers. As listed in Table I, both dendrimers displayed characteristic amide bands (amide A, B, I, II, and III) and  $\text{CH}_2$  bands (stretching, bending) and

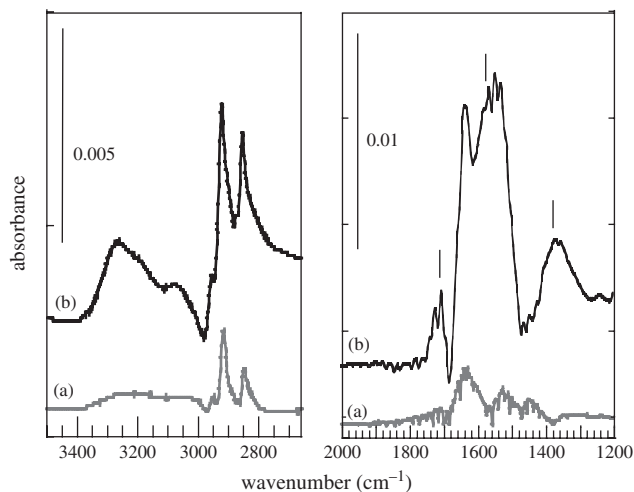


**Fig. 5.** Transmission SEIRAS of dendrimer adlayers prepared at 15 min adsorption from aqueous solutions (0.01 wt%). (a) G4 amine hydrochloride-terminated poly(amido amine) dendrimer; (b) G2.5 carboxylate-terminated poly(amido amine) dendrimer.

a C–C stretching band. Additionally, carboxyl-terminated PAMAM dendrimer has C=O and C–O stretching bands from COOH and  $\text{COO}^-$  stretching bands. This means coexistence of COOH and  $\text{COO}^-$  species. It is apparent from the comparison of absorbance that adsorption of carboxyl-terminated PAMAM dendrimers is more abundant than that of amine-terminated PAMAM dendrimers.

SEIRAS at the adsorption equilibrium are shown in Figure 6 for carboxyl-terminated PAMAM dendrimer at different pHs. Absorbance of  $\text{COO}^-$  stretching vibration bands (~1580 and ~1400  $\text{cm}^{-1}$ ) decreased below pH 6 and, instead, the absorbance of C=O (COOH) stretching band (~1710  $\text{cm}^{-1}$ ) increased. However, weak

**Table I.** Transmission SEIRA bands (in  $\text{cm}^{-1}$ ) and their assignments of dendrimer adlayers prepared at 15 min adsorption from aqueous solutions (0.01 wt%) of G4 amine hydrochloride-terminated and G2.5 carboxylate-terminated poly(amido amine) dendrimers.<sup>a</sup>

Amine hydrochloride-terminated	Carboxylate-terminated	Assignment
vw	3259m	amide A (NH stretching + overtone)
vw	3060w	amide B (NH stretching + overtone)
2918m	2917m	$\text{CH}_2$ antisymmetric stretching
2849m	2846m	$\text{CH}_2$ symmetric stretching
	1711w	C=O(COOH) stretching
1640m	1640s	amide I (C=O stretching)
	1580sh	$\text{COO}^-$ antisymmetric stretching
1547w	1547s	amide II (NH in-plane bending + C–N stretching) $\text{CH}_2$ bending (scissoring)
1439w	1374m	$\text{COO}^-$ symmetric stretching, $\text{CH}_2$ bending (wagging)
	1240w	C–O(COOH) stretching
	1188m	amide III (C–N stretching + NH in-plane bending)
	1013m	C–C stretching

<sup>a</sup>s, strong; m, medium; w, weak; vw, very weak; sh, shoulder.

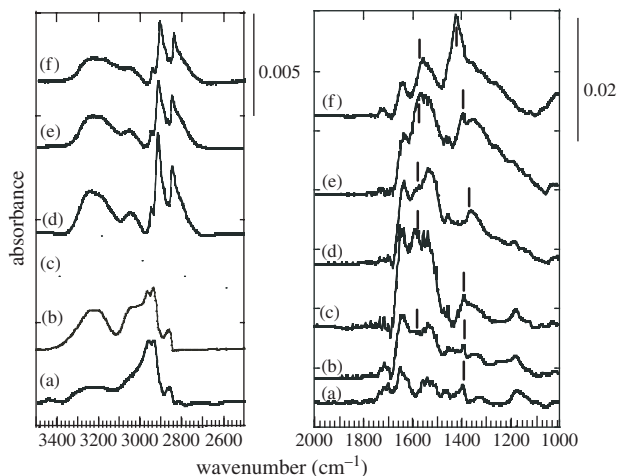


**Fig. 6.** Transmission SEIRAS of dendrimer adlayers prepared at 30 min adsorption from aqueous solutions (0.01 wt%) of G2.5 carboxyl-terminated poly(amido amine) dendrimer at different pHs. (a) pH 1.40; (b) pH 4.06; (c) pH 6.50; (d) pH 9.98; (e) pH 11.73; (f) pH 12.89.

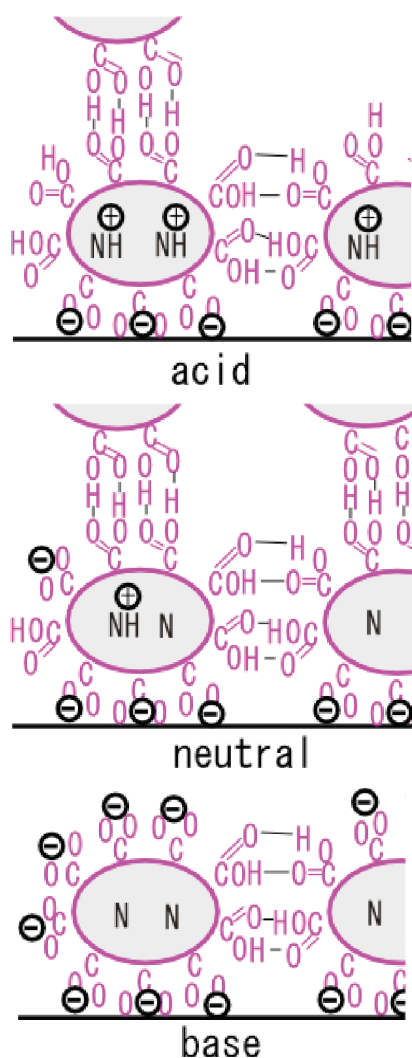


**Fig. 7.** Schematic illustration of G2.5 carboxyl-terminated poly(amido amine) dendrimer adsorbed on gold substrate at different pH regions.

COO<sup>-</sup> bands were observed even at acidic pH. At the same time, amide I and II, which were overlapped on COO<sup>-</sup> bands at alkaline and neutral pHs, became distinguishable at acidic pH.

The situation of dendrimer molecules in adsorption film at equilibrium on gold substrate is schematically illustrated in Figure 7 on ground of pK values of dendrimer (tertiary amine and terminal carboxylate) and the results described above. In alkaline solution, since the terminal groups of dendrimer are deprotonated, dendrimers are bound on a substrate through carboxylate ions at the monolayer adsorption state. Additional adsorption does not occur because of electrostatic repulsion between charged dendrimers. When pH came close neutral, some of protonated tertiary amines coexist with deprotonated carboxylate terminals, and the neutralization happens. This brings on the adsorption of dendrimers on dendrimer monolayer owing to less hydrophilicity of dendrimer and/or hydrogen bonding between coexisting carboxylic acid terminals of dendrimers. At this situation, adlayer thickens. At acidic pH, whole tertiary amines in dendrimer are protonated and electrostatic repulsions disturb adsorption of dendrimer on dendrimer monolayer. Additional adsorption (1 ~ 2 monolayers) can occur due to the hydrogen bonding between carboxylic acids of dendrimers. On the desorption process at whole pHs, almost of adlayers are removed except the first monolayer, which strongly interacts with substrate through terminal deprotonated carboxylates of dendrimers.

#### 4. CONCLUSIONS

In the present study, we confirmed that carboxylate derivatives of PAMAM dendrimers can form self-assembled monolayers on metal substrates due to adsorption from aqueous solution and rinse with water. Since the resultant self-assembled monolayer is stable at whole pH region from acid to alkaline, this dendrimer self-assembled monolayer prepared by one-pot method should be expected the utilization as a functional film.

#### References and Notes

1. F. Zeng and S. C. Zimmerman, *Chem. Rev.* **97**, 1681 (1997).
2. M. Fischer and F. Vögtle, *Angew. Chem. Int. Ed.* **38**, 884 (1999).
3. V. Percec and M. N. Holerca, *Biomacromolecules* **1**, 6 (2000).
4. J. P. Kampf, C. W. Frank, E. E. Malmström, and C. J. Hawker, *Langmuir* **15**, 227 (1999).
5. S. Watanabe and S. L. Regen, *J. Am. Chem. Soc.* **116**, 8855 (2000).
6. (a) T. Imae, M. Ito, K. Aoi, K. Tsutsumiuchi, H. Noda, and M. Okada, *Colloid Surfaces, A-Phys. Eng. Asp.* **175**, 225 (2000); (b) M. Ito, T. Imae, K. Aoi, K. Tsutsumiuchi, H. Noda, M. Okada, *Langmuir*, **18**, 9757 (2002).
7. (a) O. Yemul, M. Ujihara, N. Maki, and T. Imae, *Polymer J.* **37**, 82 (2005); (b) M. Ujihara and T. Imae, *J. Colloid Interface Sci.*, in press.
8. V. V. Tsukruk, F. Rinderspacher, and V. N. Bliznyuk, *Langmuir*, **13**, 2171 (1997).
9. C. Li, K. Mitamura, and T. Imae, *Macromolecules* **36**, 9957 (2003).

10. (a) M. Wells and R. M. Crooks, *J. Am. Chem. Soc.* 118, 3988 (1996); (b) H. Tokuhisa and R. M. Crooks, *Langmuir* 13, 5608 (1997).
11. (a) H. Nagaoka and T. Imae, *Trans. Mater. Res. Soc. Jpn.* 26, 945 (2001); (b) H. Nagaoka and T. Imae, *Int. J. Nonlinear Sci. Numer. Simul.* 3, 223 (2002).
12. T. Yamazaki and T. Imae, *J. Nanosci. Nanotechnol.* 5, 1066 (2005).
13. (a) M. Zhao, H. Tokuhisa, and R. M. Crooks, *Angew. Chem. Int. Ed. Engl.* 36, 2596 (1997); (b) W. M. Lackowski, J. K. Campbell, G. Edwards, V. Chechik, and R. M. Crooks, *Langmuir* 15, 7632 (1999).
14. C. B. Gorman, R. L. Miller, K.-Y. Chen, A. R. Bishop, R. T. Haasch, and R. G. Nuzzo, *Langmuir* 14, 3312 (1998).
15. (a) Z. Bo, L. Zhang, B. Zhao, X. Zhang, J. Shen, S. Höppener, L. Chi, and H. Fuchs, *Chem. Lett.* 1197 (1998); (b) L. Zhang, F. Huo, Z. Wang, L. Wu, X. Zhang, S. Höppener, L. Chi, H. Fuchs, J. Zhao, L. Niu, and S. Dong, *Langmuir* 16, 3813 (2000).
16. S. S. Sheiko, A. I. Buzin, A. M. Muzafarov, E. A. Rebrov, and E. V. Getmanova, *Langmuir* 14, 7468 (1998).
17. C. Hirano, T. Imae, S. Fujima, Y. Yanagimoto, and Y. Takaguchi, *Langmuir* 21, 272 (2005).
18. M. Ujihara, J. Orbulescu, T. Imae, and R. M. Leblanc, *Langmuir* 21, 6846 (2005).
19. D. J. Díaz, G. D. Storrier, S. Bernhard, K. Takada, and H. D. Abruña, *Langmuir* 15, 7351 (1999).
20. T. Yamazaki, T. Imae, H. Sugimura, N. Saito, K. Hayashi, and O. Takai, *J. Nanosci. Nanotechnol.* 5, 1792 (2005).
21. (a) Z. Zhang and T. Imae, *Nano Lett.* 1, 241 (2001); (b) Z. Zhang, N. Yoshida, T. Imae, Q. Xue, M. Bai, J. Jiang, and Z. Liu, *J. Colloid Interface Sci.* 243, 382 (2001); (c) T. Imae, T. Niwa, Z. Zhang, *J. Nanosci. Nanotechnol.* 2, 37 (2002).
22. (a) Z. Zhang and T. Imae, *J. Colloid Interface Sci.* 233, 99 (2001); (b) Z. Zhang and T. Imae, *J. Colloid Interface Sci.* 233, 107 (2001); (c) T. Imae, in *Encyclopedia of Surface and Colloid Science*, Marcel Dekker, 3547 (2002).
23. (a) H. Raether, *Surface Plasmons on Smooth and Rough Surfaces and on Gratings*, Springer Tracts in Modern Physics, Springer-Verlag, Berlin (1988), Vol. 111; (b) J. M. Phelps and D. M. Taylor, *J. Phys. D: Appl. Phys.* 29, 1080 (1996).
24. H. Nagaoka and T. Imae, *J. Colloid Interface Sci.* 264, 335 (2003).
25. T. Imae, T. Takeshita, and K. Yahagi, *Studies of Surface Science and Catalysis*, 132, 477 (2001).

Received: 15 October 2005. Accepted: 25 November 2005.

Delivered by Publishing Technology to: University of Waterloo  
IP: 184.183.1.206 On: Sun, 01 Nov 2015 08:54:51  
Copyright: American Scientific Publishers